ENDOR Study of Copper(II) Crown Porphyrin Dimerization

Hans van Willigen* and T. K. Chandrashekar†

Contribution from the Department of Chemistry, University of Massachusetts at Boston, Boston, Massachusetts 02125. *Received June 24, 1985*

Abstract: An ENDOR study was made of the effect of dimerization on the ligand hyperfine and quadrupole interactions in copper *meso*-5,10,15,20-tetrakis(benzo-15-crown-5)porphyrin (CuTCP). ENDOR spectra from triplet state $[CuTCP]_2$ give direct access to signs and magnitudes of hyperfine components. It is found that dimerization reduces the ^{14}N hyperfine tensor components by a factor of 2 and leaves the quadrupole couplings unaffected. This shows that the structure of CuTCP is not changed appreciably upon dimerization. The hyperfine and quadrupole data are in agreement with a dimer structure in which the copper nuclei are placed on a common axis normal to the planes of the porphyrins. The magnitude of the effect of intermolecular dipole–dipole coupling on the in-plane proton hyperfine component is consistent with a Cu–Cu separation of 0.42 nm. The [CuTCP] ENDOR spectra establish that the three ^{14}N and two in-plane ^{1}H hyperfine tensor components are positive. The data from this study of CuTCP and $[CuTCP]_2$ randomly oriented in frozen solution are in close agreement with those obtained in a single crystal ENDOR study of CuTPP.

Thanabal and Krishnan[1,2] recently reported on the synthesis and properties of free base and metallo tetraphenylporphyrins with crown ether substituents (*meso*-5,10,15,20-tetrakis(benzo-15-crown-5)porphyrin (I)). It was shown that addition of certain cations (for instance K^+ and NH_4^+) to solutions of these crown porphyrins induces dimerization. From the stoichiometry of the reaction it can be deduced that four crown–cation–crown linkages join the two porphyrins in a parallel configuration. Dimers of VOTCP and CuTCP in frozen solution give ESR spectra characteristic for axially symmetric molecules with a triplet ground state.[3] From a measurement of the value of the zero-field splitting (zfs) parameter D it is deduced that the center-to-center distance between the porphyrin planes in $[CuTCP]_2$ must be about 0.42 nm.[1]

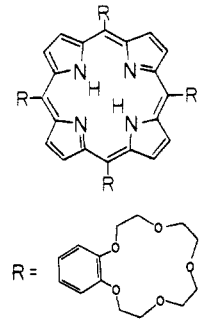

I. TCP

This paper is concerned with an electron nuclear double resonance (ENDOR) study of the monomers and dimers of CuTCP. It has been shown[4-7] that ENDOR measurements on triplet state molecules randomly oriented in solid solution can give detailed information on hyperfine and quadrupole interactions. The application of the technique on the crown porphyrins is of some interest for a number of reasons. First, the measurements can provide supporting evidence for the geometric structure proposed for the dimers. Second, information on the values of proton and nitrogen hyperfine coupling constants will give an insight into the effect of dimerization on the delocalization of the unpaired electrons. Third, the method makes it possible to determine the signs of hyperfine coupling constants.[4-7] Hence, it can give direct information on the mechanism of spin density delocalization.

To our knowledge this is the first reported ENDOR study of dimers of a paramagnetic transition-metal complex. Dimers of transition-metal complexes are found in many systems of biological interest.[8] The results presented here demonstrate that the technique can provide valuable data on the structure of such systems.

† Present address: Department of Chemistry, Michigan State University, East Lansing, MI.

Experimental Section

The synthesis of CuTCP followed the procedures reported in the literature.[1,2] ESR and ENDOR spectra were recorded with a VARIAN E-9 X-band ESR spectrometer equipped with a home-built ENDOR accessory interfaced to a Nicolet 1180E computer.[9,10] ENDOR spectra were recorded at temperatures between 10 and 20 K with an Oxford Instruments E9 helium cryostat. Typical conditions used for recording the spectra were the following: microwave power 5 mW, radio frequency power 200 W, 10 kHz FM with a deviation of ±50 kHz. Field modulation was not used in recording ENDOR signals. Spectra are presented as first derivatives of the absorption signal. The computer was used for data acquisition as well as simulation of ENDOR spectra. Simulated spectra were obtained by diagonalizatin of the complete spin Hamiltonian matrix followed by calculation of the moments of nuclear spin transitions. In the case of powder spectra simulated spectra represent the sum of contributions calculated at one degree intervals for the range of relevant orientations. A Lorentzian line shape was assumed in the calculations. Samples were made up of CuTCP ($\sim 10^{-3}$ M) in a toluene–chloroform (1:1) or methanol–chloroform (1:1) solvent mixture. Dimerization was induced by the addition of KCl ($\sim$10-fold excess) to the solutions. In the recording of proton ENDOR spectra use was made of deuterated solvents in order to eliminate resonance peaks from solvent protons. Solvents were used as received from commercial sources. To verify peak assignments some measurements were performed on copper tetraphenylporphyrin (CuTPP) in polycrystalline ZnTPP and on frozen solutions of phenyl-deuterated CuTPP.

Results

ESR. Figure 1 shows the rigid matrix ESR spectra of the monomer and dimer of CuTCP. As is well-documented,[11] the characteristic shape of the monomer spectrum is due to the anisotropy in the **g** and metal ion hyperfine tensor. The perpendicular region of the spectrum shows structure due to hyperfine interaction with the porphyrin nitrogens. Figure 1b illustrates that addition of KCl ($\sim 10^{-2}$ M) generates an ESR spectrum characteristic for triplet state molecules with axial symmetry.[3] The zfs parameter D is 380 G which corresponds to a center-to-center distance between the porphyrins of about 0.42 nm.[1] For the interpretation of the ENDOR data it is important to note that the exchange

(1) Thanabal, V.; Krishnan, V. *J. Am. Chem. Soc.* **1982**, *104*, 3643.
(2) Thanabal, V.; Krishnan, V. *Inorg. Chem.* **1982**, *21*, 3606.
(3) Chang, C. K. *J. Heterocycl. Chem.* **1977**, *14*, 1285.
(4) van Willigen, H.; Mulks, C. F. *J. Chem. Phys.* **1981**, *75*, 2135.
(5) van Willigen, H.; Kirste, B.; Kurreck, H.; Plato, M. *Tetrahedron* **1982**, *38*, 759.
(6) Kirste, B.; van Willigen, H. *Chem. Phys. Lett.* **1982**, *92*, 339.
(7) van Willigen, H.; Chandrashekar, T. K. *J. Chem. Phys.* **1983**, *78*, 7093.
(8) For a review see: Boas, J. F.; Pilbrow, J. R.; Smith, T. D. In "Biological Magnetic Resonance"; Berliner, L. J., Reuben, J., Eds.: Plenum: New York, 1978; Vol. 1, Chapter 7.
(9) Mulks, C. F.; van Willigen, H. *J. Phys. Chem.* **1981**, *85*, 1220.
(10) Kirste, B.; van Willigen, H. *J. Phys. Chem.* **1982**, *86*, 2743.
(11) Manoharan, P. T.; Rogers, M. T. In "Electronic Spin Resonance of Metal Complexes"; Teh Fu Yen, Ed.: Plenum: New York, 1969.

0002-7863/86/1508-0709$01.50/0

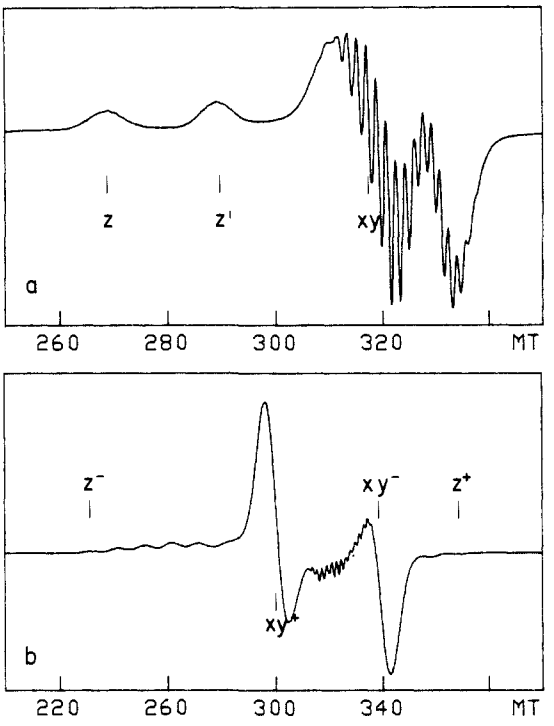

Figure 1. Frozen solution ESR spectra of (a) CuTCP ($\sim 10^{-3}$ M) and (b) CuTCP ($\sim 10^{-3}$ M) with added KCl ($\sim 10^{-2}$ M): solvent, methanol–chloroform (1:1); temperature, 10 K; field sweep (a) 100 mT, (b) 200 mT; field modulation 10 G, microwave power 5 mW; sweep time 5 min.

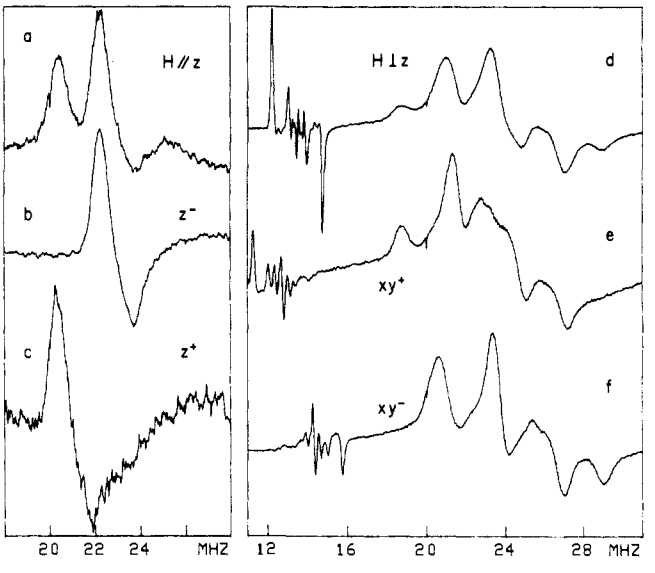

Figure 2. ^{14}N ENDOR spectra obtained with the z (a) and xy (d) field settings marked in Figure 1a (monomer) and the z^- (b), z^+ (c), xy^+ (e), and xy^- (f) field settings marked in Figure 1b (dimer). The H$\perp z$ spectra (d–f) show proton ENDOR signals in the frequency region below 16 MHz. Temperature 10 K, microwave power 5 mW, fm 50 kHz. The spectra represent the time average of 1000 (H$\|z$) and 500 (H$\perp z$) 1–s sweeps.

interaction between the unpaired electrons is larger than the metal ion hyperfine coupling. As a consequence, the hyperfine coupling is one-half the value in the monomer.[12] Also the number of hyperfine peaks increases because the unpaired electrons interact with two (equivalent) Cu nuclear spins rather than one. The $[CuTCP]_2$ spectrum does not show superhyperfine structure.

^{14}N ENDOR. Figure 2a depicts the ^{14}N ENDOR spectrum obtained with the magnetic field (H) set on the peak labeled z (cf. Figure 1a) of the CuTCP ESR spectrum. With this field

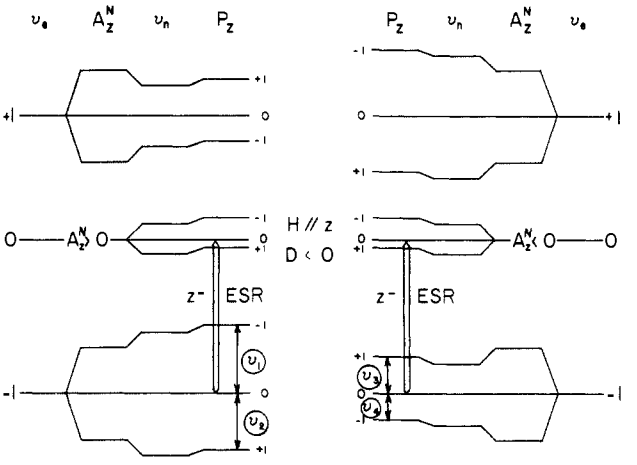

Figure 3. Schematic energy level diagram for an electron spin 1–nuclear spin 1 system in a magnetic field. The nine spin states are affected by the electron Zeeman interaction and dipole–dipole interaction between the unpaired electrons (ν_e), by the hyperfine interaction (A_z^N), the nuclear Zeeman interaction (ν_N), and the quadrupole interaction (P_z). The diagram represents the case that $D < 0$ and illustrates the effect of a change in sign of A_z^N on the ordering of the energy levels. Hyperfine shifted ENDOR transitions that can be observed with the z^- field setting are labeled ν_1, ν_2 ($A_z^N > 0$), and ν_3, ν_4 ($A_z^N < 0$).

setting an ENDOR signal is obtained of molecules oriented so that H is normal to the porphyrin plane.[11] Ignoring second-order effects, ^{14}N is expected to give rise to a pair of peaks separated by $2\nu_N$ and centered around $1/2|A_z^N|$. Here ν_N denotes the nuclear Zeeman frequency and A_z^N the z component of the hyperfine tensor. Quadrupole interaction may give rise to a further splitting of the peaks. The ^{14}N spectrum shown in Figure 2a consists of a pair of broad lines centered around 21.9 MHz, displaying signs of unresolved structure. The separation of the peaks corresponds approximately to $2\nu_N$ (1.67 MHz). From the peak positions it is deduced that $|A_z^N| = 43.8$ MHz. It has been shown previously that second-order effects due to the presence of magnetically equivalent ^{14}N nuclei gives rise to a series of up to 14 nuclear spin transitions.[13] However, even in single crystal measurements the H$\|z$ spectrum is only partly resolved. The single crystal spectrum shows two broad lines with some structure centered around $1/2|A_z^N|$.[13] In the measurements reported here a restricted range of orientations around H$\|z$ is probed. The resulting line broadening obliterates virtually all structure. The z component (P_z) of the quadrupole tensor cannot be derived from the spectrum.

ENDOR spectra obtained with the field set on the peaks labeled z^- and z^+ in the ESR spectrum of the dimer (cf. Figure 1b) are given in Figure 2, b and c. In this case the field settings select the molecular orientations contributing to the ENDOR spectra as well as the electron spin manifolds within which nuclear spin transitions are induced. In these "biradical type" dimers with unpaired electrons largely confined to the metal ions D must be negative.[4,5] Figure 3 gives a schematic energy level diagram for an electron spin 1, nuclear spin 1 (^{14}N) system with $D < 0$ for the case that $A_z^N > 0$ or $A_z^N < 0$. The diagram shows that for $D < 0$ the low-field ESR lines (z^-) represent transitions between the −1 and 0 electron spin states of molecules oriented so that H$\|z$. The high-field ESR lines (z^+) are due to $0 \leftrightarrow +1$ electron spin transitions. Ignoring second-order effects, ^{14}N NMR transitions in the $M_s = 0$ spin manifold will be found at $\nu_N \pm {}^3/_2P_z$. These transitions fall in the 1-MHz region, and no attempt was made to record the resonance peaks. Figure 3 illustrates that ENDOR peak positions associated with NMR transitions in the $M_s = \pm 1$ manifolds are determined in part by the sign of A_z^N. For $A_z^N > 0$ and z^- field setting ($M_s = -1$), peak positions are given by $A_z^N + \nu_N \pm {}^3/_2P_z$, with the z^+ field setting ($M_s = +1$) the peaks shift to $A_z^N - \nu_N \pm {}^3/_2P_z$. For $A_z < 0$ the ENDOR line positions obtained with the two field settings are interchanged. *It follows*

(12) Reitz, D. C.; Weissman, S. I. *J. Chem. Phys.* **1960**, *33*, 700.

(13) Brown, T. G.; Hoffman, B. M. *Mol. Phys.* **1980**, *39*, 1073.

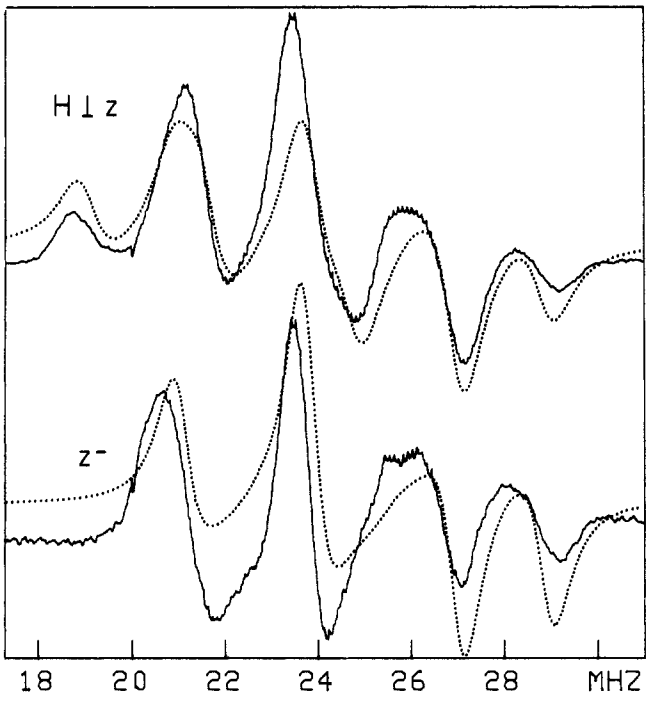

Figure 4. Top: H⊥z ^{14}N ENDOR spectrum of CuTCP (solid line) with computer-simulated spectrum (dotted line). Bottom: ^{14}N ENDOR spectrum from $[CuTCP]_2$ with the field set on the xy^- peak in the ESR spectrum (cf. Figure 1b). Hyperfine and quadrupole coupling constants used in the simulations are given in Table I. Temperature 10 K, microwave power 5 mW, fm 50 kHz. The experimental spectra are the time average of 500 1-s sweeps.

that the ENDOR spectra give direct information on the sign of the hyperfine coupling. Figure 2 shows that ^{14}N resonance frequencies obtained with the z^- and z^+ field settings correspond to the high and low frequency peak positions in the monomer spectrum. Two conclusions can be drawn from this observation. First, $|A_z^N|$ in the dimer must be one-half $|A_z^N|$ in the monomer. Second, the sign of A_z^N must be positive.

^{14}N ENDOR spectra obtained with the xy field settings in the ESR spectra of CuTCP and $[CuTCP]_2$ (cf. Figure 1, a and b) are given in Figure 2, d–f. With these field settings NMR transitions are observed in molecules oriented so that H lies in the porphyrin plane (H ⊥ z).[11] As a consequence, a two-dimensional powder pattern is observed. Since the detection technique generates the first derivative of the absorption spectrum, one expects to observe peaks for the two orientations where H lies along an extreme of the in-plane ^{14}N hyperfine interaction. For the monomer, ENDOR frequencies in a first-order approximation are given by $1/2|A_i^N| \pm \nu_N \pm 3/2P_i^N$, where i (=x or y) labels the two in-plane principal axes of the hyperfine tensor. Of the eight peaks five are clearly resolved in the monomer spectrum given in Figure 2d. Values of $|A_i^N|$ and P_i^N, were extracted from the spectrum with the aid of the single crystal data on CuTPP reported by Brown and Hoffman,[13] and computer simulations. The values are given in Table I. In the ESR spectrum of $[CuTCP]_2$ (cf. Figure 1b) the xy^- and xy^+ field settings correspond *primarily* to orientations for which H⊥z. With the high field (xy^-) setting NMR transitions in the $M_s = -1$ manifold are recorded, whereas transitions in the $M_s = +1$ manifold are observed with the low field (xy^+) setting. For $A_i^N > 0$ hyperfine shifted ENDOR peaks are found at $|A_i^N| + \nu_N \pm {}^3/_2P_i^N$ (xy^- setting) or $|A_i^N| - \nu_N \pm {}^3/_2P_i^N$ (xy^+ setting). Again the line positions are interchanged if $A_i^N < 0$. By using as a starting point the in-plane quadrupole tensor components and *half* the in-plane hyperfine components found for CuTPP,[13] a satisfactory simulation of the experimental spectra was obtained by minor adjustments of the parameters. Figure 4 displays experimental and simulated ^{14}N spectra for monomer (xy field setting) and dimer (xy^- field setting). The experimental spectra contain contributions from orientations other than H⊥z. The simulations do not take this into account. Also second-order effects due to the presence of equivalent ^{14}N's are ignored. This accounts for differences between experimental and computer generated spectra. Hyperfine and quadrupole data derived from the spectra are given in Table I.

Proton ENDOR. Proton ENDOR spectra obtained with the field settings discussed earlier are presented in Figure 5. With the z field setting in the monomer ESR spectrum only one pair

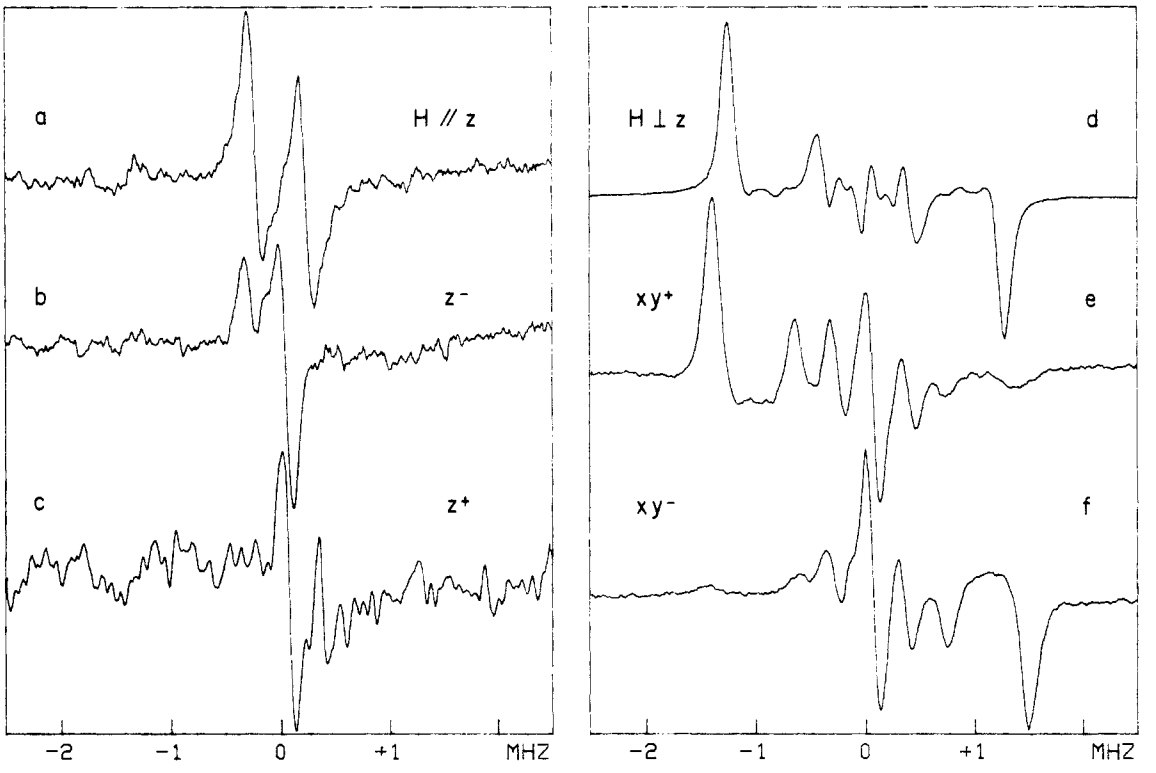

Figure 5. Proton ENDOR spectra from CuTCP (a, d) and $[CuTCP]_2$ (b, c, e, f) for H||z (left) and H⊥z (right). The frequency scale is given relative to the proton Zeeman frequency. Temperature 10 K, microwave power 5 mW, fm 50 kHz. Spectra are the time average of 2000 (H||z) and 500 (H⊥z) 1-s sweeps.

Table I

system	nucleus	A_x	A_y	A_z	P_x	P_y	P_z
CuTCP[a]	^{14}N	53.8	42.8	44.1	−0.66	+0.89	
$[CuTCP]_2$[a]	^{14}N	+26.9	+21.4	+22.0	−0.66	+0.89	
CuTPP/ZnTPP[b]	^{14}N	+54.213	+42.778	+44.065	−0.619	+0.926	−0.307
CuTCP	^{1}H	2.47	0.70	0.44			
$[CuTCP]_2$	^{1}H	+1.43	+0.29	−0.32			
CuTPP/ZnTPP[b]	^{1}H	+2.47	+0.70	+0.80			
CuTPP[c]	^{1}H	+2.47	+0.70	+0.44			

[a] The measurements give the relative signs of P_x and P_y only. [b] Data from a single crystal ENDOR study.[13] The study give the *relative* signs of the hyperfine components and the quadrupole components. [c] Relative signs derived from a computer analysis of the ENDOR spectra, see text.

of lines is observed (Figure 5a) centered around the proton Zeeman frequency (ν_p) and separated by 0.44 MHz. The same result is obtained with CuTPP in frozen toluene-d_8–$CDCl_3$ and in polycrystalline ZnTPP. Deuteration of the phenyl rings does not affect these resonance peaks. It is concluded that they must be due to the pyrrole protons.

Since $\nu_p > A_i^H$, each set of equivalent protons in CuTCP will give rise to a pair of peaks at $\nu_p \pm {}^1/_2 A_i^H$, where i represents the molecular axis along which the field is pointed. In $[CuTCP]_2$ the z^- and xy^- field settings will generate ENDOR peaks at ν_p and $\nu_p + A_i^H$, the z^+ and xy^+ field settings at ν_p and $\nu_p - A_i^H$ ($i = x$, y, or z). The z^- and z^+ ENDOR spectra given in Figure 5, b and c, indeed show a peak at ν_p and one hyperfine shifted peak. For the z^- field setting the hyperfine shifted line is found at a lower frequency than ν_p. The peak shifts to a higher frequency for the z^+ setting. This observation establishes that the z component of the hyperfine tensor (A_z^H) in the dimer must be negative. Its value is −0.32 MHz.

The two-dimensional powder spectra (xy field settings) are given in Figure 5, d–f. Measurements on phenyl-deuterated CuTPP establish that the phenyl protons make only minor contributions to the proton ENDOR spectra. For this reason the hyperfine shifted peaks found in the powder ENDOR spectra of CuTCP and $[CuTCP]_2$ are attributed to the pyrrole protons. The powder spectra give signs and magnitudes of the extremes of the in-plane hyperfine interaction (A_x^H, A_y^H). Computer simulations based on the data given in Table I account quite well for the major features in the experimental spectra. It should be noted that with the xy field settings orientations differing from $H \perp z$ can make significant contributions. This is especially true in the case of $[CuTCP]_2$, where $-1 \leftrightarrow 0$ electron spin transitons overlap with $0 \leftrightarrow 1$ transitions in the xy^- and xy^+ regions of the ESR spectrum.

Discussion

Thanabal and Krishnan proposed[1,2] that the crown ether porphyrin dimers have a structure in which the porphyrins are face-to-face and the two metal ions are positioned on a common axis normal to the porphyrin planes. The ENDOR data fully support the proposed structure. One expects that a deviation from coplanarity or shift of the porphyrin planes with respect to each other would show up clearly in the ENDOR spectra. First, because this perturbs the axial symmetry of the system and will induce an inequivalence of nitrogens and of pyrrole protons. Second, in a system that deviates from the proposed model the **g** and metal ion hyperfine tensor axes will not be colinear with the zfs tensor axes. As a consequence, the orientations probed with the z and xy field settings in the monomer ESR spectra will differ from those in the dimer ESR spectra. This will be reflected in changes in measured hyperfine couplings that cannot be accounted for on the basis of the proposed geometry. Dimerization could induce a shift of the position of the metal ion relative to the four surrounding nitrogen atoms without perturbing the fourfold symmetry. However, such a change is expected to affect spin delocalization to the nitrogens and would modify the ^{14}N hyperfine tensor components. The ^{14}N data for $[CuTCP]_2$ show no evidence of such as effect. Within experimental evidence the measured ^{14}N hyperfine splitting constants are one-half the values found for the monomer. The factor of 2 reduction shows that the electronic structure of the CuTCP molecules is essentially unperturbed. The fact that the quadrupole couplings do not show a dimerization effect supports this conclusion.

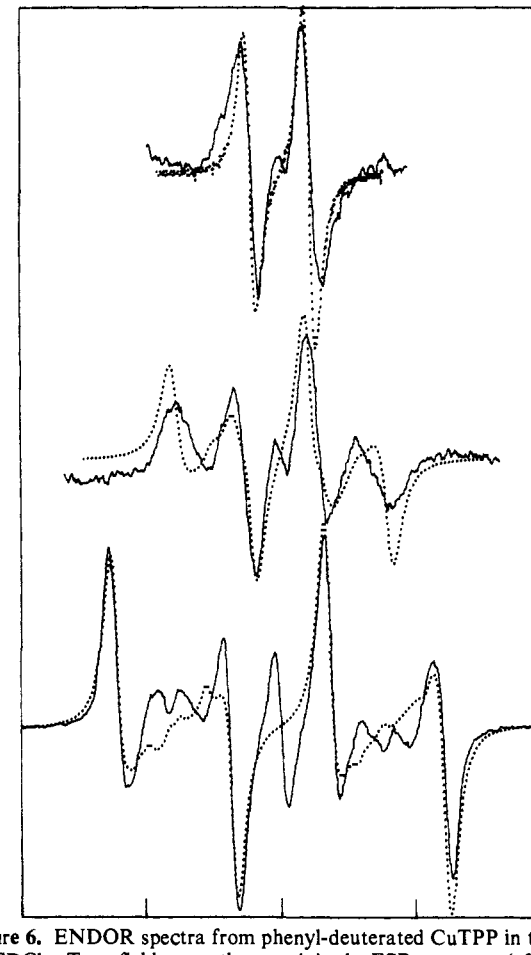

Figure 6. ENDOR spectra from phenyl-deuterated CuTPP in toluene-d_8–$CDCl_3$. Top: field set on the z peak in the ESR spectrum (cf. Figure 1a). Middle: z' field setting. Bottom: xy field setting. Simulated spectra are given by the dotted lines. A discussion of the computer analysis is given in the text. Temperature 10 K, microwave power 5 mW, fm 50 kHz. Experimental spectra are the time average of 1000 ($H \| z$) and 500 ($H \perp z$) 1-s sweeps.

Table I shows that the proton hyperfine interaction components do not show the factor of 2 reduction. A_x^H can be measured quite accurately so that for this parameter the deviation is definitely outside the error limits. For the in-plane components (A_x^H, A_y^H) the deviations can be attributed to the dipole–dipole interaction between the electron spin on one ring and the pyrrole protons associated with the other ring. The magnitude of this effect can be estimated by using a point-dipole model. With a center-to-center distance between the porphyrins of 0.42 nm[1] and a Cu–H distance of 0.52 nm,[13] the intermolecular dipole–dipole coupling adds about 0.2 MHz to A_x^H and reduces A_y^H by half that amount. If a correction is made for this intermolecular contribution the factor of 2 relationship is found for these parameters as well.

There are a number of problems with the values found for A_z^H in CuTCP and $[CuTCP]_2$. First, it is noteworthy that A_z^H in CuTCP (0.44 MHz) differs from that found for CuTPP doped in single crystals of ZnTPP (0.80 MHz).[13] As noted before,

samples of CuTPP in frozen solution and polycrystalline ZnTPP gave the same H||z ENDOR spectrum as CuTCP. Therefore, the discrepancy is not due to a difference in sample composition. Second, the study by Brown and Hoffman[13] established that the three components of the proton hyperfine tensor have the same sign. By contrast, in $[CuTCP]_2$ A_x^H, $A_y^H > 0$ and $A_z^H < 0$. An analysis of the ENDOR spectra from phenyl-deuterated CuTPP in frozen toluene-d_8–$CDCl_3$, on the other hand, leads to the conclusion that A_x^H, A_y^H, $A_z^H > 0$. Figure 6 shows spectra obtained with z, z', and xy field settings (cf. Figure 1a). Computer-calculated spectra are given by the dotted lines. Computer simulations of the xy spectrum established unequivocally that A_x^H and A_y^H must have the same sign. With the z' setting, the ENDOR spectrum contains contributions from the $H||z$ orientation as well as from molecules oriented so that H lies on a cone making an angle of approximately 50° with the molecular z axis. The shape of this spectrum is sensitive to the relative signs of all three hyperfine components. It was found that only a calculation based on the assumption that the three components have the same sign gives a result that fits the experimental spectrum. It is hard to conceive of a mechanism that would cause the A_z^H value of the pyrrole protons to change sign upon going from CuTCP to $[CuTCP]_2$. The possibility that the hyperfine shifted peaks in the z^- and z^+ spectra are not due to the pyrrole protons cannot be excluded and this seems to offer the most satisfactory explanation for the results.

Table I shows that, except for the A_z^H data, the results obtained in this study closely match those reported for CuTPP.[13] Apparently the introduction of the crown ether groups does not perturb the electronic structure of the Cu porphyrin core. The single crystal measurements show that the three ^{14}N hyperfine tensor components must have the same sign. The same conclusion is reached with regards to the proton hyperfine tensor components. The theoretical analysis presented by Brown and Hoffman[13] is based on the assumption that the hyperfine coupling components are all positive. The ENDOR study of $[CuTCP]_2$ provides evidence that this is correct. It is noteworthy that the ENDOR study of phenyl-deuterated CuTPP demonstrates that information on *relative* signs can be derived from spectra of samples in powders or frozen solution as well.

Acknowledgment. Thanks are due to Dr. U. Das for assistance in some of the measurements. Financial support by the Division of Chemical Sciences, Office of Basic Energy Sciences of the Department of Energy under contract DE-FG02-84ER13242, is gratefully acknowledged.

Kinetics and Mechanism of the Alkylnickel Formation in One-Electron Reductions of Alkyl Halides and Hydroperoxides by a Macrocyclic Nickel(I) Complex

Andreja Bakac* and James H. Espenson*

Contribution from the Ames Laboratory and Department of Chemistry, Iowa State University, Ames, Iowa 50011. *Received July 8, 1985*

Abstract: The nickel(I) macrocycle Ni(1*R*,4*R*,8*S*,11*S*-tmc)$^+$ (tmc = 1,4,8,11-tetramethyl-1,4,8,11-tetraazacyclotetradecane) reacts readily with primary alkyl halides in alkaline aqueous solutions, yielding alkylnickel(II) complexes, $RNi(tmc)^+$. The reaction is proposed to occur in two steps, the first and rate-limiting being one-electron transfer from $Ni(tmc)^+$ to RX, either by halogen atom transfer or outer-sphere electron transfer, to yield an alkyl radical R·. The latter is captured by $Ni(tmc)^+$ in a second and more rapid reaction. This mechanism is supported by the nature of the alkylnickel complexes produced, by the reactivity order within a series of alkyl halides (methyl < primary < secondary), and by the trapping of the carbon-centered radical $CH_2CH(CH_2)_3CH_2$· in competition with its cyclization. Free radicals are also involved in the formation of alkylnickel complexes in reactions of $Ni(tmc)^+$ with alkyl hydroperoxides. No organonickel formation is observed in reactions with benzyl bromide, whereas benzyl chloride yields the short-lived $PhCH_2Ni(tmc)^+$. The steady-state concentration of benzyl radicals in the faster $PhCH_2Br$ reactions is too high to allow significant coupling with $Ni(tmc)^+$ in competition with the radical self-reaction. With 2-propyl halides the alkylnickel complex is also not formed because radical coupling occurs in preference to the Ni–C bond formation owing to steric reasons.

Reactions of alkyl halides with reduced metal ions are among the most convenient synthetic routes for the preparation of organotransition-metal complexes. The great interest in these reactions lies additionally in the variety of mechanisms involved in the metal–carbon bond formation. A distinction among a halogen atom transfer,[1-6] electron transfer,[7] or oxidative addition[8-13] is usually possible on the basis of the reactivity order within a series of alkyl halides, detailed product analysis, trapping of radical intermediates, and stereochemistry around the α-carbon.

The rich chemistry of nickel and its importance in catalytic processes have prompted a number of studies of the reduction of alkyl halides by nickel complexes. These reactions are generally characterized by a multiplicity of reaction pathways and a diversity

(1) Davis, D. D.; Kochi, J. K. *J. Am. Chem. Soc.* **1964**, *86*, 5264.
(2) Kochi, J. K.; Powers, J. W. *J. Am. Chem. Soc.* **1970**, *92*, 137.
(3) Chock, P. B.; Halpern, J. *J. Am. Chem. Soc.* **1969**, *91*, 582.
(4) Halpern, J. *Ann. N.Y. Acad. Sci.* **1974**, *239*, 2.
(5) Samuels, G. J.; Espenson, J. H. *Inorg. Chem.* **1979**, *18*, 2587.
(6) Kupferschmidt, W. C.; Jordan, R. B. *J. Am. Chem. Soc.* **1984**, *106*, 991.
(7) Marzilli, L. G.; Marzilli, P. A.; Halpern, J. *J. Am. Chem. Soc.* **1970**, *92*, 5752.
(8) Schrauzer, G. N.; Deutsch, E. *J. Am. Chem. Soc.* **1969**, *91*, 3341.
(9) Collman, J. P.; MacLaury, M. R. *J. Am. Chem. Soc.* **1974**, *96*, 3019.
(10) (a) Hart-Davis, A. J.; Graham, W. A. G. *Inorg. Chem.* **1970**, *9*, 2658. (b) Hart-Davis, A. J.; Graham, W. A. G. *Ibid.* **1971**, *10*, 1653.
(11) (a) Clark, H. C.; Manzer, L. E. *Inorg. Chem.* **1973**, *12*, 362. (b) Brown, M. P.; Puddephatt, R. J.; Upton, C. E. E. *J. Chem. Soc., Dalton Trans.* **1974**, 2457.
(12) Lau, K. S. Y.; Wong, P. K.; Stille, J. K. *J. Am. Chem. Soc.* **1976**, *98*, 5832.
(13) Collman, J. P.; Finke, R. G.; Cawse, J. N.; Brauman, J. I. *J. Am. Chem. Soc.* **1977**, *99*, 2515.

0002-7863/86/1508-0713$01.50/0